Heat treatment effects on LPBF duplex stainless steel corrosion resistance

Zbigniew Brytan[1], Mengistu Dagnaw[1]

1Department of Engineering Materials and Biomaterials, Faculty of Mechanical Engineering, Silesian University of Technology, ul. Konarskiego 18a, 44-100, Gliwice, Poland

The LPBF-manufactured super duplex stainless steel (SDSS) was subjected to stress-relieving and solution annealing heat treatments and was tested in as printed conditions. The main objective of the study was to verify the corrosion resistance of SDSS by Tafel polarisation and electrochemical impedance spectroscopy in a chloride-rich solution. Structural analysis was performed by LOM/SEM and X-ray diffraction. The correlation between corrosion resistance, microstructure, and heat treatment was evaluated.

As a result of the very fast cooling rate of the LPBF process, the SDSS reveals ferrite as the major phase in the as printed conditions, similarly after stress relieving at 300°C/5h. Ferrite grains are elongated in the building direction with some austenite precipitation along the grain boundaries. Solution annealing leads to a well-balanced phase composition, with austenite evenly distributed among ferritic grains. This transformation positively affects corrosion resistance. Notably, both the polarisation resistance (Tafel analysis) and the charge transfer resistance (EIS) consistently highlighted the improved corrosion resistance of solution annealed SDSS. The stress relieving at 300°C/5h of LPBF SDSS slightly improves electrochemical parameters when analysing anodic polarisation curves, while a more notable increase in charge transfer resistance was evidenced in the EIS test, compared to as-printed SDSS.

Keywords: *LPBF, super duplex stainless steel, heat treatment, corrosion resistance*

1. Introduction

Duplex Stainless Steels (DSS) are renowned for their unique ability to combine ferritic stainless steels' strengths with austenitic stainless steels' toughness. They are widely recognised for their exceptional mechanical properties, superior corrosion resistance, and cost-effectiveness. Super Duplex Stainless Steel (SDSS) and Hyper Duplex Stainless Steel (HDSS) have garnered significant interest in the realm of Laser Powder Bed Fusion (LPBF) and additive manufacturing (AM). With a higher alloy content, these advanced steel grades offer improved mechanical properties and enhanced corrosion resistance compared to standard duplex stainless steel (DSS). Achieving the desired mechanical and corrosion resistance properties requires establishing a balanced austenite-ferrite structure.

Moreover, with increase of alloying elements (Cr, Mo, Ni, etc.) in SDSS, HDSS, the risk of precipitation of secondary phases also increases (Fig.1), which influence the toughness and corrosion properties [1)].

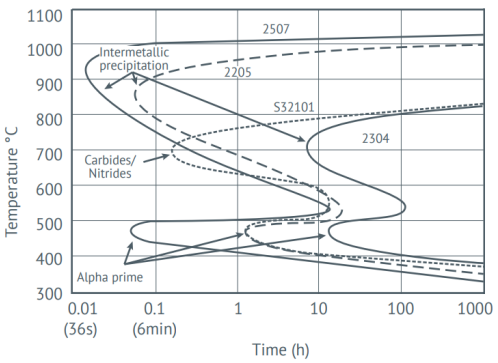

Figure 1. Isothermal precipitation diagram for various DSS.

In contrast, fusion-based additive manufacturing processes experience rapid sequences of heating, melting, solidification, and cooling due to their distinctive layer-by-layer deposition approach [1)]. As duplex stainless steel compositions were initially formulated for conventional manufacturing processes, the intricate thermal cycles in AM pose challenges in achieving a well-balanced ferrite/austenite microstructure, affecting the final properties. A comparable analogy to the microstructures seen in additively manufactured duplex stainless steels is found in the fusion zone microstructures of autogenously welded duplex stainless steels. These microstructures are predominantly ferritic with minimal austenite, located primarily at grain boundaries and interspersed within the ferritic matrix, along with limited intragranular austenite [2)].

As mentioned above, due to its rapid cooling rate, LPBF presents challenges in this regard, often resulting in a predominantly ferritic microstructure in as-printed condition [3)]. To address this limitation, post-processing annealing becomes necessary to achieve a well-balanced duplex microstructure. Moreover, stress-relief annealing can be further applied after additive manufacturing to optimise the microstructure and properties of DSS components.

Recent literature on additive manufacturing of DSS, i.e., HDSS, addresses such issues [4-6)]. The evolution of microstructures, mechanical properties and corrosion resistance of AM HDSS (UNS S32707) was comprehensively investigated by Shang et al. [3)]. As printed microstructure of HDSS, SDSS apart from fully ferritic may also contain precipitations of secondary phases, like sigma [3)], chromium nitrides [3)]. However, appropriate solution annealing, with a well-designed soaking time, results in a balanced ferrite-austenite microstructure with optimal fine grain size.

Stress relieving is another option to minimize residual stresses and enhance the material's mechanical properties in as-build conditions. Stress relieving also results in dimensional stability and reduced risk of deformation or cracking during service of AM components. The stress relieving treatment is generally not recommended for DSS because they are prone to the formation of detrimental and unwanted phases at the temperatures that may normally be considered for stress relieving (i.e., 500°C to 800°C). The maximum service temperature of all DSS grades is limited to below 315°C, according to ASME pressure vessel codes,

and other codes specify even lower service temperatures, as low as 250°C for SDSS.

For the above reasons, it was decided to investigate the effect of heat treatment - stress relieving at 300°C/5h, which will be safe for causing undesirable microstructural changes in the duplex stainless steel microstructure and may improve the properties of the material compared to the as-printed one. Finally, three states of printed SDSS were compared, i.e., in the as-printed conditions, after stress-relieving and after solution annealing. The main focus was to evaluate and compare the corrosion resistance of LPBF SDSS.

2. Experiment

The super duplex stainless steel gas atomised powder with particle diameters ranging 15 - 45 µm, grade 2507, of Sandvik Osprey Ltd, with the following chemical composition 25%Cr, 7%Ni, 4%Mo, <1.2%Mn, <0.8Si, <0.3%N, <0.5%Cu, <0.03%C, <0.035%P and <0.015%S, was printed with the LPBF method.

The AM125 Renishaw printer was used with the following parameters: laser power of 180W, hatch distance of 120 µm, layer thickness of 30 µm, and scan speed of 300 mm/s, giving the energy density of 166 J/mm^3 during printing. A meander scanning strategy (67°) was used. Horizontal samples were printed as for the Charpy impact test (10x10x55mm). Microstructural studies and corrosion tests were performed in the cross section.

The samples were then subjected to post-processing heat treatment: stress relieving at 300°C/5h with slow cooling with the furnace and solution annealing at 1100°C/15min with fast cooling in water. The as-printed samples were also studied without any post-processing heat treatment.

X-ray diffraction patterns were collected on X-Pert PRO instrument, using a Co lamp, and the X'Pert HighScore Plus software was used for phase identification. The samples for microstructural observations, LOM, and SEM were electrolytically etched in 10% oxalic acid, 3-5 V, 15-30 s.

Corrosion resistance was studied using potentiodynamic polarisation and electrochemical impedance spectroscopy (EIS) on an Atlas 0531EU & IA (Atlas-Sollich) potentiostat station in 3.5% NaCl solution at room temperature. The reference electrode of Ag/AgCl was used and Pt wire as the auxiliary electrode. The Tafel extrapolation, according to the Stern–Geary equation, was applied to determine characteristic electrochemical parameters in AtlasLab software. The breakdown potential (E_{br}) and the repassivation potential (E_{rp}) were determined by analysing anodic polarisation curves.

Electrochemical impedance spectroscopy (EIS) tests were performed by recording changes in resistance and impedance in the variable frequency range (100 kHz - 0.01 Hz) by signal of 10 mV. The. An electrical equivalent circuit (EEC) was adopted where impedance $Z=R_s+(CPE_1+R_{ct})$, was assigned to reproduce behaviours ongoing on the sample's surface. The R_s represents solution resistance, CPE_1 capacitance, and R_{ct} is the charge transfer resistance that may be directly linked to the corrosion resistance of the surface.

3. Results and Discussion

The as-printed super duplex stainless steel SDSS revels almost fully ferritic structure due to the rapid cooling rate of 10^6-10^8°C/s in LPBF process. The X-ray diffraction pattern (Fig. 2) shows, only one weak peak deriving from the austenite – Fe-γ (111). The heat treatment of stress relieving at 300°C/5h also does not change the ferritic nature of the printed SDSS. The phase content after solution annealing 1100°C/15min become balanced and strong peaks from austenite and ferrite are visible in the XRD pattern.

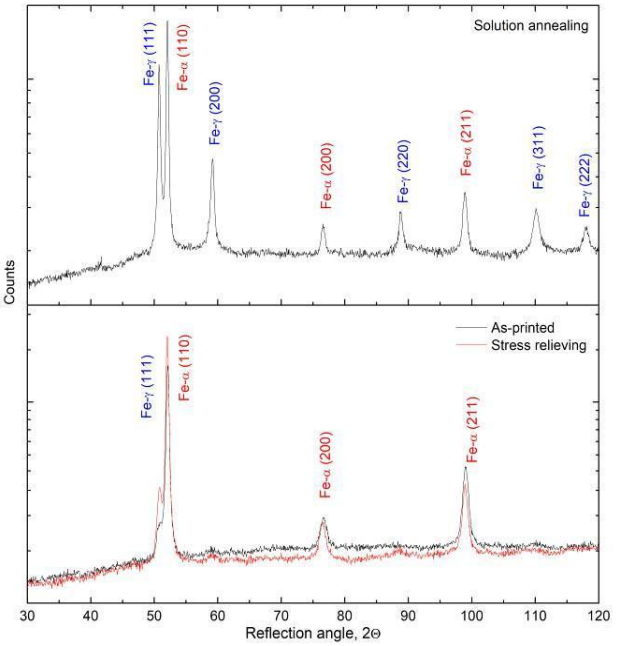

Figure 2. The XRD patterns of as-printed, stress relieved and solution annealed SDSS.

The microstructural observations of as printed and stress relieved SDSS revelled uniform ferritic grains distribution, related to heat dissipation and scanning strategy typical in AM process (Fig. 3). Austenite was hardly identified on the primary ferritic grains.

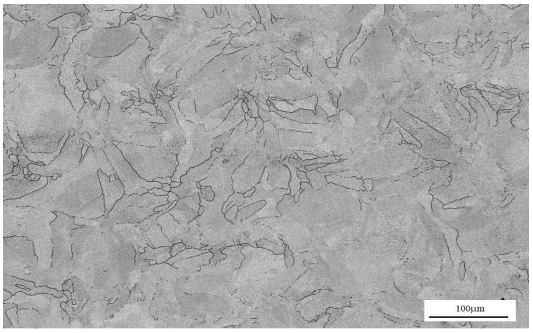

Figure 3. The microstructure of SDSS in as-printed conditions, SEM.

In the case of solution annealed SDSS (Fig. 4) the balanced fine ferritic-austenitic microstructure was formed.

The studied heat treatment conditions greatly influence the corrosion resistance of AM SDSS (Tab. 1). As expected, solution annealing increases corrosion resistance,

the polarisation resistance (R_{pol}) increased from 126mv to 149mv compared to the as printed conditions, the open circuit potential (E_{ocp}) shifted towards positive values. The balanced two-phase structure has better corrosion characteristics than a microstructure composed mainly of ferrite. In the case of stress relieving, there was a slight improvement in electrochemical parameters compared to the state after printing. This is due to the lack of structural changes and the structure of steel with a dominant share of ferrite. All of SDSS undergo repassivation when reversing current polarisation. The solution annealed SDSS also repassivated faster than other heat treatment conditions.

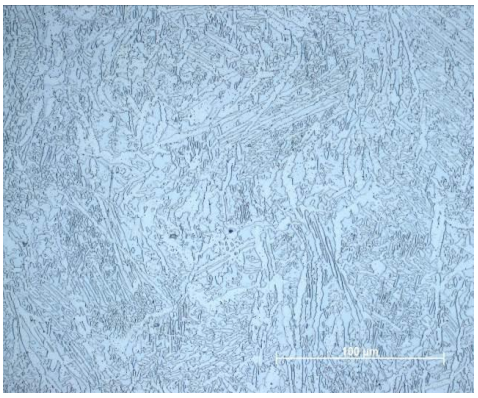

Figure 4. The microstructure of SDSS in solution annealing conditions, LOM.

Table 1. The electrochemical parameters of LPBF SDSS

Heat treatment conditions	E_{OCP}	J_{corr}	E_{corr}	R_{pol}	E_{br}	E_{rep}
	mV	μA/cm^2	mV	Ω*cm^2	mV	mV
As printed	- 966	140.63	-147.17	126.82	1084	923
Stress relieving	- 955	166.60	-142.86	125.14	1083	955
Solution Annealing	-835	131.89	-136.35	149.35	1102	1090

Comparable results were obtained in the EIS test (Table 2), where the increase in corrosion resistance, analysed based on charge transfer resistance (R_{ct}), was much greater after solution annealing. The EIS results indicated an almost double corrosion resistance of SDSS in solution-annealed condition compared to that of the as printed one. The material in the stress relieving state was also characterised by 20% higher corrosion resistance than in the as-printed state.

Table 2. The EIS parameters of LPBF SDSS

Heat treatment conditions	R_S	*CPE1*		R_{ct}
	Ω·cm^2	*Y*	*n*	Ω·cm^2
		10-6 μF cm^{-2}	-	
As printed	7.98	83.61	0.70	78.34
Stress relieving	6.95	49.57	0.70	94.80
Solution Annealing	13.55	70.25	0.77	121.50

The non-uniform distribution of residual stresses may result in varying corrosion rates across the material's surface. Stress relieving aids in achieving a more uniform stress distribution, which could lead to enhanced and consistent corrosion resistance. Residual stresses have the potential to initiate and advance localised corrosion, such as pitting and crevice corrosion. Stress relieving can help mitigate stress-related factors contributing to localized corrosion vulnerabilities.

The obtained results indicate that the use of stress relieving at 300°C/5h does not significantly improve the corrosion resistance, probably some of the internal stresses have been eliminated, which will be confirmed in subsequent tests of mechanical properties and impact toughness. In terms of corrosion resistance, it is worth performing tests of LPBF SDSS after stress-relieving heat treatment at higher temperatures, considering the temperature-time range of secondary phase precipitations.

4. Conclusions

In its initial as-printed and stress-relieved states, Laser Powder Bed Fusion (LPBF) Super Duplex Stainless Steel (SDSS) exhibits a microstructure that is primarily ferritic with limited austenite content. Solution annealing leads to a well-balanced phase composition, with austenite evenly distributed among ferritic grains. This transformation positively affects corrosion resistance. Notably, both the polarisation resistance (R_{pol}) and charge transfer resistance (R_{ct}) consistently highlighted the improved corrosion resistance of solution annealed SDSS. The stress relieving at 300°C/5h of LPBF SDSS slightly improve electrochemical parameters when analysing anodic polarisation curves, while more notable increase in charge transfer resistance was evidenced in EIS test, comparing to as-printed SDSS.

Future investigations will concentrate on refining the time-temperature parameters of the stress relieving process for LPBF-printed SDSS.

Acknowledgments

The research presented in this work received great support from the EU-project H2020-MSCA-RISE-2018 Number 823786, i-Weld, and international project co-financed by the programme of the Ministry of Science and Higher Education entitled "PMW" in the years 2020 - 2023; contract No. 5107/H2020/2020/2.

References

1) J. Fritz, Practical guide to using duplex stainless steels (10044), Nickel Institute, 2020.
2) V. Muthupandi, P. Bala Srinivasan, V. Shankar, S.K. Seshadri, S. Sundaresan, Mater. Lett. 59 (2005) 2305–2309.
3) T.A. Palmer, Stainless Steel World Publisher -May 6, 2022, https://stainless-steel-world.net/
4) A. Mulhi, S. Dehgahi, P. Waghmare, A.J. Qureshi, Metals 13 (2023) 725.
5) F. Shang, X. Chen, Z. Wang, Z. Ji, F. Ming, S. Ren, X. Qu, Metals 2019, 9, 1012.
6) K. Davidson, S. Singamneni, Mater. Manuf. Process. 31 (2016) 1543–1555.
7) S. Papula, M. Song, A. Pateras, X-B. Chen, M. Brandt, M. Easton, Y. Yagodzinskyy, I. Virkkunen, H. Hänninen, Materials 12 (2019) 2468.